VOL. 17, NO. 24, DECEMBER 2022 ISSN 1819-6608
ARPN Journal of Engineering and Applied Sciences

www.arpnjournals.com

IMPROVE AND ANALYZE THE PERFORMANCE OF PHOTOVOLTAIC SYSTEMS CONTROLLED BY AN ADVANCED FUZZY LOGIC METHOD FOR FAST AND STABLE MPPT

Yassine El Moujahid[1], Abdessamad Benlafkih[2], Abdelkader Hadjoudja[3] and Nadia El Harfaoui[1]
[1]Laboratory of Material Physics and Subatomic, Faculty of Sciences, Ibn-Tofail University, BP, Kenitra, Morocco
[2]Advanced Systems Engineering Laboratory, Ibn-Tofail University, BP, Kenitra, Morocco
[3]Laboratory of Electronic Systems, Information Processing, Mechanics and Energetics, Faculty of Sciences, University Ibn-Tofail, BP, Kenitra, Morocco
E-Mail: yassine.elmoujahid@uit.ac.ma

ABSTRACT

The main problem that often arises in photovoltaic systems is to achieving the maximum output power and maintaining the DC-DC connection voltage at a stable value since the power generated by photovoltaic panels is very powerless in uncertain climatic conditions. Moreover, the sunshine and temperature constantly change during the day. The aim of this work is to adapt and optimize an intelligent control algorithm for photovoltaic systems based on a fuzzy logic method to track the maximum power point (MPPT) at a stable value with a fast settling time and to optimize the efficiency under different influences of weather conditions (lighting and temperature). The system consists of a photovoltaic solar module connected to a DC-DC boost converter and a load. The effectiveness of the proposed system was validated by computer simulations using MATLAB/Simulink software. The results of this work show that the efficiency of the photovoltaic system can be improved up to 99.1% by using the advanced fuzzy logic controller.

Keywords: photovoltaic system PV, model solar, fuzzy logic controllers, pulse width modulation (PWM), boost converter, maximum point power tracking algorithm (MPPT).

1. INTRODUCTION

Photovoltaic energy sources are considered a clean form of energy generation that is environmentally friendly and saves energy at the lowest cost and with increased efficiency. It offers one of the most efficient ways of energy generation, with real prospects for the present and future. Improving the efficiency of the photovoltaic (PV) generator, in other words, maximizing the power delivered to the load connected to the generator terminals. It's important to improve the DC/DC converters, where the converters act as an interface between the PV source and the load. In order to track the MPP and thus operate the GPV system at its maximum power point (MPP), a maximum power point tracking (MPPT) controller is used [1, 2].

We can divide the design of the PV system into two parts: the PV array modeling and the MPPT DC-DC boost converter, which is present at the output of the PV generator to produce the maximum power from the PV solar modules for the load at a certain brightness and temperature. The modeling is shown in (Figure-1).

The charge controller incorporates the maximum power point tracking (MPPT) algorithm to extract the maximum available power from the PV modules under certain conditions. The realization of the MPPT controller is based on different techniques and algorithms such as:

- The Perturbation and Observation (P&O) method [3, 4].
- Incremental Conductance (IC) method [5].
- Integral Proportional (IP) method [6].
- Constant Voltage (CV) method [7].
- Short Circuit Current [8].
- Fuzzy Logic (FL) method [9].
- Fuzzy Logic Type 2 (FL 2) method [1].
- Cuckoo Search (CS) method [10].

In this work, the modification of the intelligent control of a photovoltaic system based on fuzzy logic was made and verified to ensure the maximum power point tracking with a fast response time and at a stable value under different influences of climatic conditions (lighting and temperature).

2. PHOTOCOLTAIC SYSTEM MODEL

The photovoltaic system consists of a photovoltaic panel, converter DC-DC (boost), control system, and Load as shown in (Figure-1).

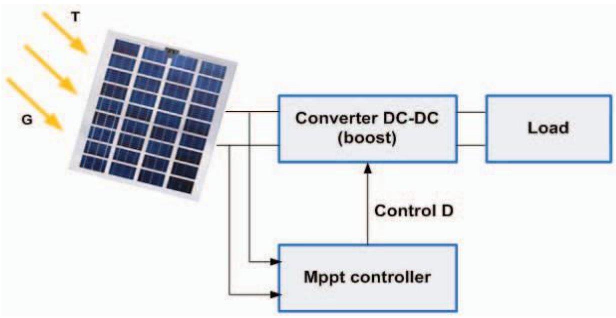

Figure-1. Photovoltaic system.

ARPN Journal of Engineering and Applied Sciences

Photovoltaic (PV) systems absorb sunlight and convert it into electricity. The load is connected to the output of the boost converter. The PV solar system operates in both Maximum Power Point Tracking and derated Voltage Control modes.

2.1 Photovoltaic Cell Model

PV cells and modules are the key components of PV systems, which absorb photons of light and release electron charges, and can directly convert solar energy into electricity [11]. The common and popular PV models are single diodes and double diodes [12]. Here, we use the single diode D which represents the P-N junction to describe the characteristics of PV cells [13].

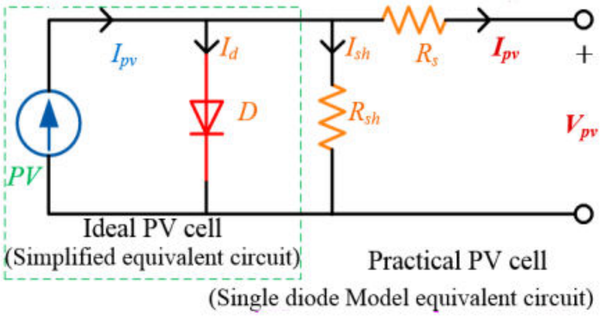

Figure-2. Equivalent circuit of the photovoltaic (PV) cell.

The single diode equivalent circuit is shown in (Figure-2), where D is a parallel diode, Rsh is the shunt resistance and Rs is the series resistance. The output mathematical equations were obtained in References [11, 14, & 15].

$$I_{pv} = I_{ph} - I_d - I_{R_{sh}} \tag{1}$$

$$I_{pv} = I_{ph} - I_0\left[\exp\left(\frac{q(V_{pv}+R_sI_{pv})}{AKT}\right) - 1\right] - \frac{V_{pv}+R_sI_{pv}}{R_{sh}} \tag{2}$$

- The light-generated current of the elementary:

$$I_{ph} = (I_{cc} + K_i\Delta T) \tag{3}$$

- The current of the parallel diode:

$$I_d = I_0\left[\exp\left(\frac{q(V_{pv}+R_sI_{pv})}{AKT}\right) - 1\right] \tag{4}$$

I_0 is the reverse saturation current of the diode. V_{pv} and $I_{pv}$are the output voltage and current, respectively. q is the electron charge (1.602 × 10−19 C), A is the diode ideality factor, and K is the Boltzmann constant (1.38 × 10−23 J/K).

- The shunt current of resistance:

$$I_{Rsh} = \frac{V_{pv}+R_sI_{pv}}{R_{sh}} \tag{5}$$

The characteristics of the PV cell under different environmental conditions (temperature and irradiation) are shown in Figures 3 and 4. As shown by the relationship between PV output parameters and environmental variables, it is highly nonlinear and depends on the level of solar radiation and temperature changes in the PV cell [8, 9, and 16].

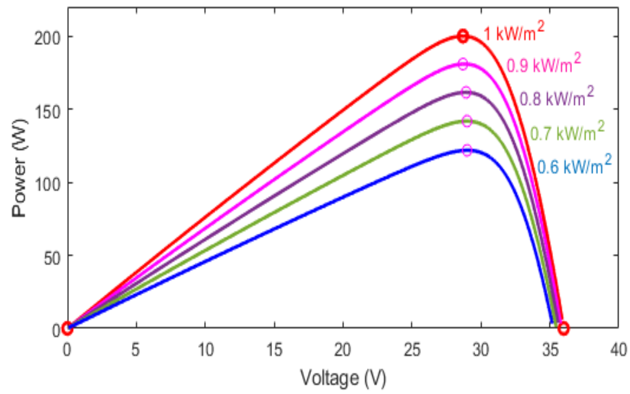

Figure-3. Different solar radiation level effect.

Figure 3, shows the curves under different radiation, i.e., the maximum power point MPP increases with radiation while the voltage Vpv increases slightly. Figure-4 shows the curves under different temperatures, i.e., that is, the maximum power point MPP decreases slightly with increasing temperatures.

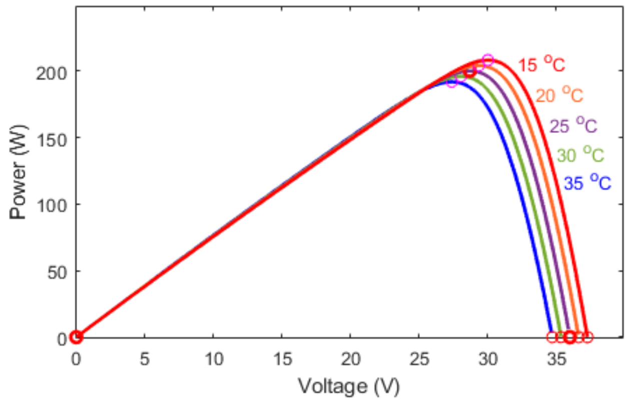

Figure-4. Different temperature variability effect.

2.2 Dc-Dc Boost Converter (Step-Up Chopper)

DC-DC converters are also known as choppers. Here we are going to take a look at the Step-Up Chopper or Boost converter which boosts the DC input voltage to a specified DC output voltage. The Boost converter consists of a DC input voltage source VA, an inductor L, a switch S, a diode D, and two capacitors Cint & Cout (Figure-5).

The DC-DC converter is an interface that enables adaptation betwixt the PV panel and the load to extract the maximum power from the panel [17, 18, & 19].

$$\frac{dI_L}{dt} = \frac{V_A}{L} \tag{6}$$

ARPN Journal of Engineering and Applied Sciences

$$\frac{dV_0}{dt} = -\frac{V_0}{C_{out}R_L} \quad (7)$$

Duty pulses are provided by the PWM pulse generator. For t between [αT, T], the transistor is off. Thereafter, T is the period of the static converter and α is the duty cycle. The converter can be modeled by the following equations:

$$\frac{dV_0}{dt} = \frac{i_L}{C_{out}} - \frac{V_0}{C_{out}R_L} \quad (8)$$

$$\frac{dI_L}{dt} = \frac{V_A - V_0}{L} \quad (9)$$

The control of the converter by a switch K (MOSFET) which can be open or closed according to the duty cycle D generated by the MPPT. [20].

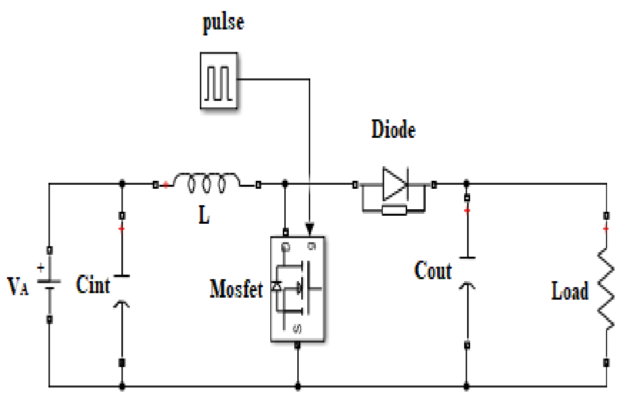

Figure-5. DC-DC boost converter.

- Duty Cycle (D):

$$D = 1 - \frac{V_A}{V_0} \quad (10)$$

- Value Of Inductor (L):

$$L \geq \frac{V_A D}{f_s \Delta I_0} \cong 5.8e-03 \text{ H} \quad (11)$$

- Capacitance (C):

$$C \geq \frac{I_0 D}{f_s \Delta V_0} \cong 4.08e-05 \text{ F} \quad (12)$$

Table-1. Boost converter parameters:

Description	Value
Frequency (fs)	1000 Hz
Nominal Resistor (Rs)	60 Ω
Inductance (L)	5.8e-03 H
Capacity (C)	4.08e-05 F
Voltage variation (ΔV)	3 %
Current variation (ΔI)	

3. THE ADVANCED FUZZY LOGIC MPPT CONTROLLER

Lotfi Zadeh's work in the sixties on fuzzy set theory and fuzzy logic, at the University of Berkeley, laid the foundations of today's fuzzy control. This work was slow to be accepted by the automation community and industry. More recently, fuzzy logic control has been used in MPPT maximum power point tracking systems. This FL control is a new approach based on artificial intelligence. According to FLC, it is an improvement of the classical CI algorithm in terms of robustness, stability, and ease of implementation. As with other MPPT controllers, the main task of the FL controller is to achieve the MPP. However, the performance of this controller mainly depends on human experience [21].

The FLC approach is based on decomposing a range of variations of a real variable into linguistic variables: "low", "medium" and "high", and assigning the membership function to each variable. The rules resulting from the human operator's expertise are expressed in linguistic form. These rules determine the dynamic performance of the FL controller.

The proposed fuzzy logic controller consists of four basic components: Fuzzification Units, Rule Base, Inference Engine, and Defuzzification (Figure-6). [22].

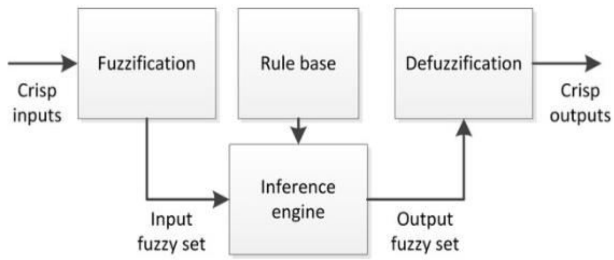

Figure-6. Fuzzy Logic Controller block diagram.

3.1 Fuzzification

The fuzzification unit is occupied with the conversion of real variables into fuzzy variables. E(k) and CE(k) are LF controller inputs given by equations (13, 14). In our case, we have two input variables which are the error E(k) and the error variation CE at instant k. The output of the FL dD controller is the variable pitch of the duty cycle.

$$E(k) = \frac{P(k) - P(k-1)}{V(k) - V(k-1)} \quad (13)$$

$$CE(k) = E(k) - E(k-1) \quad (14)$$

Figures 7, 8, and 9 show the selected membership functions of E, CE, and dD. Among the different forms of membership functions (trapezoidal, Gaussian, and triangular...), the symmetric triangular form is considered. Most suitable for its simplicity. The limits of the range of the fuzzy variables are generally normalized between -1 and +1 by introducing a gain factor to represent the real signals. In this work, the symmetric triangular shape was

ARPN Journal of Engineering and Applied Sciences

selected and the bounds are considered as ([-30, 10], [-30, 30] and [0, 1]) for (E, CE & dD) respectively.

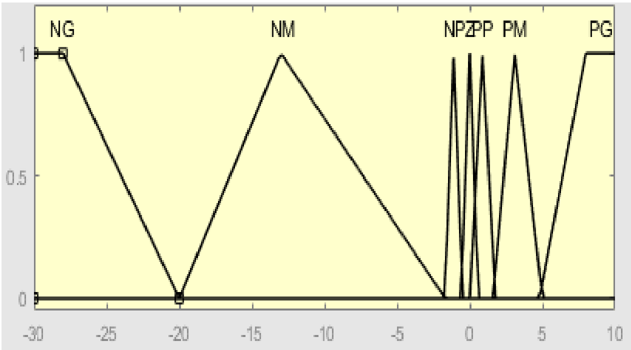

Figure-7. Input variable.

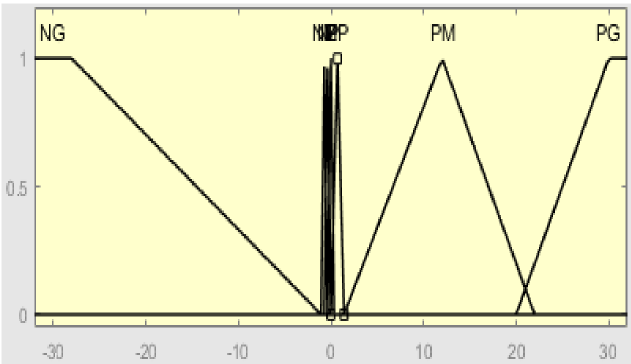

Figure-8. variable CE.

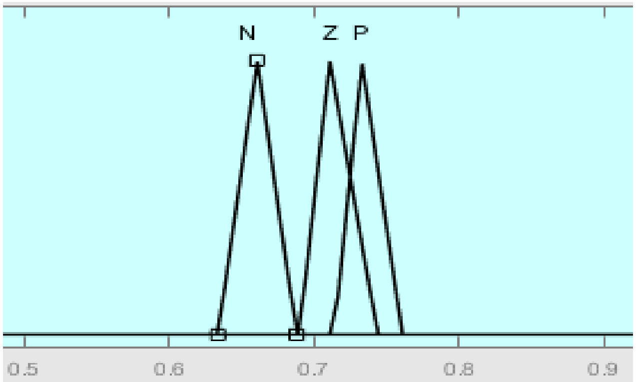

Figure-9. Output variable dD.

3.2 Fuzzy Rules Base

The ‘‘brain’’ of fuzzy logic inference, stores all ‘‘IF-THEN’’ rules that fuzzy inference required. In general, the description of these rules by experts using natural language based on their experience.

3.3 Inference Method

For obtaining the final fuzzy conclusion, according to the degree of membership of the input variables to the fuzzy sets and the detailed fuzzy rules. It exists many ways of fuzzy inference. The conclusions can be different according to the methods. Among the methods, the Mamdani inference method based on the Max-Min composition rule is generally used. Then, the table of inference rules is established in Table-2.

Table-2. Table of inference rules:

CE / E	GP	PM	PP	Z	NP	NM
GP	P	P	P	P	P	P
PM	Z	Z	Z	Z	Z	Z
PP	N	N	N	N	N	N
Z	Z	Z	Z	P	N	Z
NP	Z	Z	P	P	P	P
NM	Z	Z	Z	P	P	P

3.4 Defuzzification

The transformation step of the fuzzy output is the defuzzification subset into a non-fuzzy value that authorizes the process to be controlled. The input for the defuzzification process is a fuzzy set and the output is a unique number that needs to be applied to the system, for the final desired output as per the system a control output non-fuzzy value is required, so a defuzzification step is mandatory allowing process control. To represent the sampled data, the mean is calculated by:

$$dD = \frac{\sum_{j=1}^{n} \mu(Dj) - Dj}{\sum_{j=1}^{n} \mu(Dj)} \quad (15)$$

The output values are de-fuzzified and multiplied by the scale factor to build the current control signal (figure-6). Its role is to adjust the fuzzy controller to obtain the MPP tracking.

4. MODELING PHOTOVOLTAIC SYSTEM USING MATLAB/SIMULINK

This study employs an API156P200 photovoltaic panel. We designed and simulated our model with an innovative MPPT control based on an advanced fuzzy logic method to achieve fast and stable maximum power point tracking, as shown in (Figure-10). The voltage and current of the photovoltaic panel are used as inputs to calculate the error (E) and the error deviation (CE), which represent the input of the FL controller, as shown in (Figure-11).

VOL. 17, NO. 24, DECEMBER 2022 ISSN 1819-6608
ARPN Journal of Engineering and Applied Sciences

www.arpnjournals.com

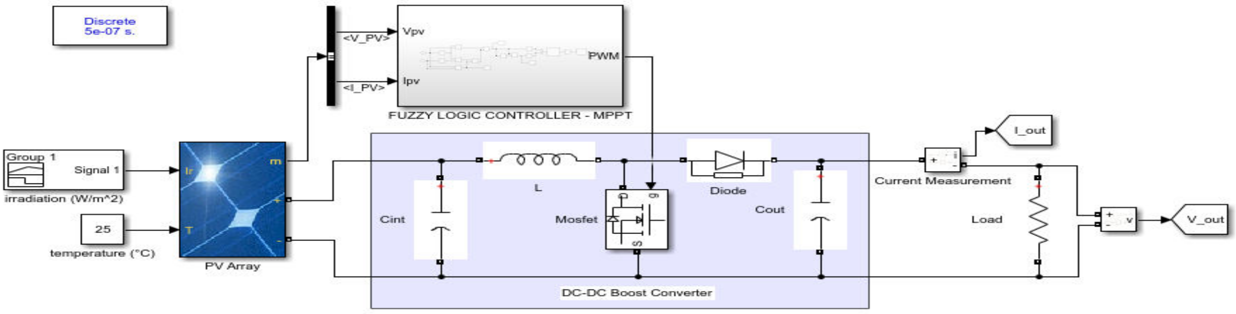

Figure-10. The glob al system in MATLAB/Simulink.

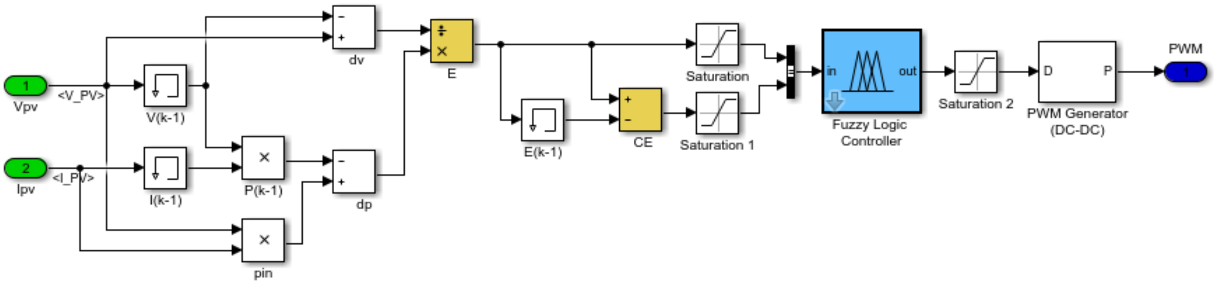

Figure-11. Schema of advanced MPPT calculator in MATLAB/Simulink.

5. RESULTS AND ANALYSIS

We can test the performance and efficiency of this advanced algorithm under different climatic conditions, we presented the input and output power of the converter at a fixed load and the voltage supplied to the outputs under increasing and decreasing illumination (1000W/m^2 to 600W/m^2 and from 600W/m^2 to 1000W/m^2) at a temperature of 25°C for 0.9 seconds, as shown in (Figure-12). Then we change the temperature from (15°C to 35°C and from 35°C to 15°C) at a fixed illuminance of 1000 W/m^2, as shown in (Figure-21). The simulation results for the proposed robust PV system were performed using MATLAB/Simulink software.

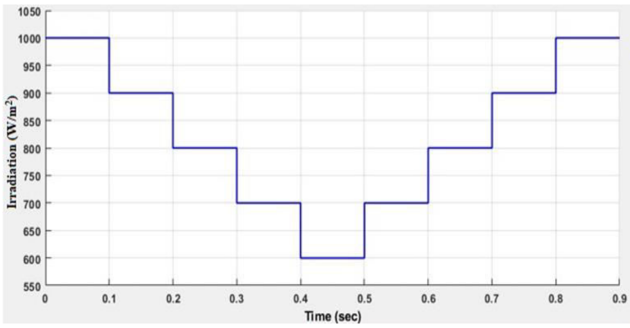

Figure-12. Change of irradiation at 25 °C.

5.1 Results with Varying Illumination at a Temperature of 25°C

Figure-13 shows the power generated by the GPV, we can observe how efficient and powerful the FL controller is to reach the MPP in fast response and remain stable with a change in brightness at a fixed temperature of 25°C, Figures (15, 17, and 19) show the simulation results of the output power, output voltage, and output current respectively, the advanced fuzzy logic system faces a fast change in illuminance, decreasing from 1000W/m^2 to 600W/m^2 and increasing from 600 W/m^2 to 1000 W/m^2 at 25°C.

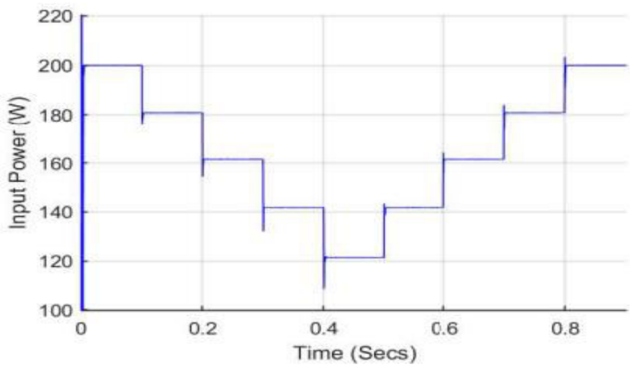

Figure-13. Input power at 25°C.

VOL. 17, NO. 24, DECEMBER 2022 ISSN 1819-6608
ARPN Journal of Engineering and Applied Sciences

www.arpnjournals.com

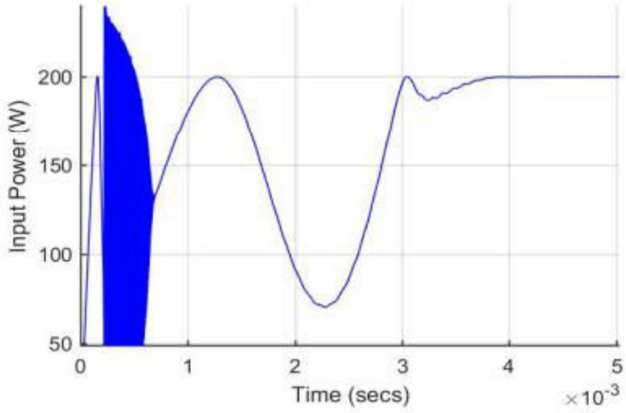

Figure-14. The zoomed image of the input power at 1000W/m^{2}at 25°C.

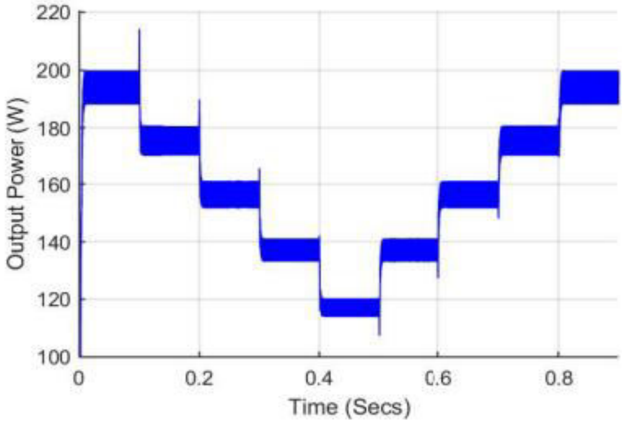

Figure-15. Output power at 25°C.

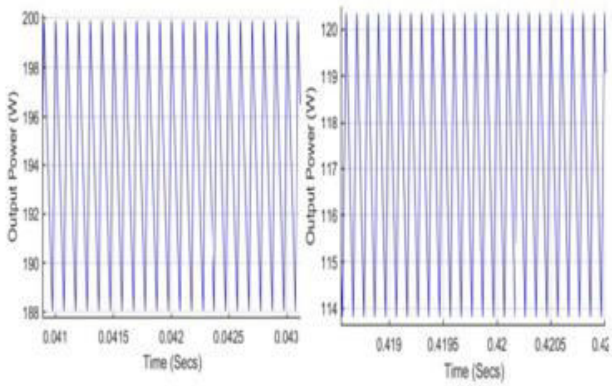

Figure-16. The zoomed image of the output power at 1000W/m^2 and 600W/m^2.

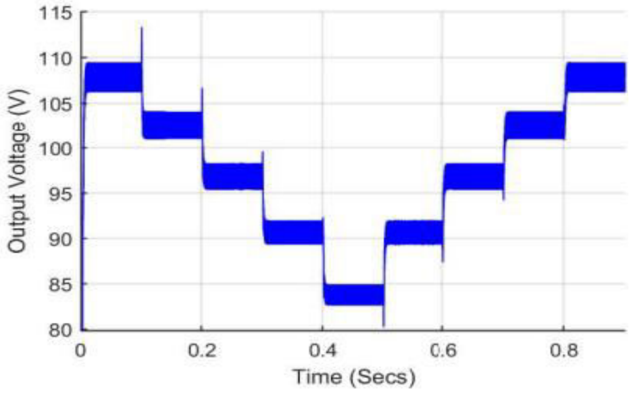

Figure-17. Output voltage at 25°C.

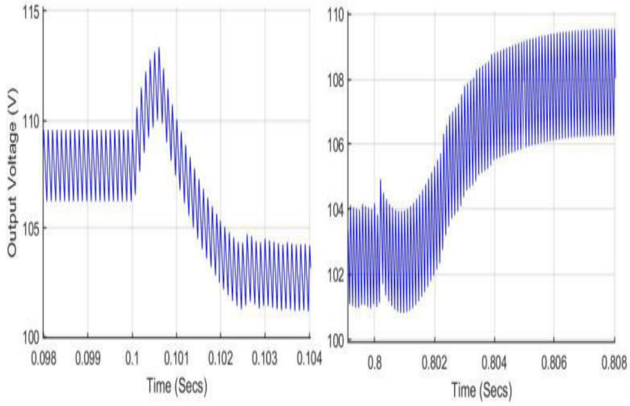

Figure-18. The zoomed image of the output voltage at 25°C.

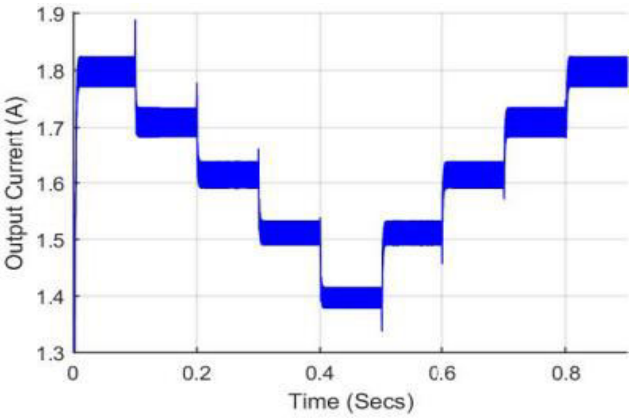

Figure-19. Output current at 25°C.

The system operates robustly with a weak ripple in a permanent state as shown in (Figures 16 and 18), low overshoot, and a fast response time of about 4 ms. as shown in (Figure-14).

Figure-20 below shows the oscillating power output with a fast settling time of about 8.5 ms.

ISSN 1819-6608
ARPN Journal of Engineering and Applied Sciences

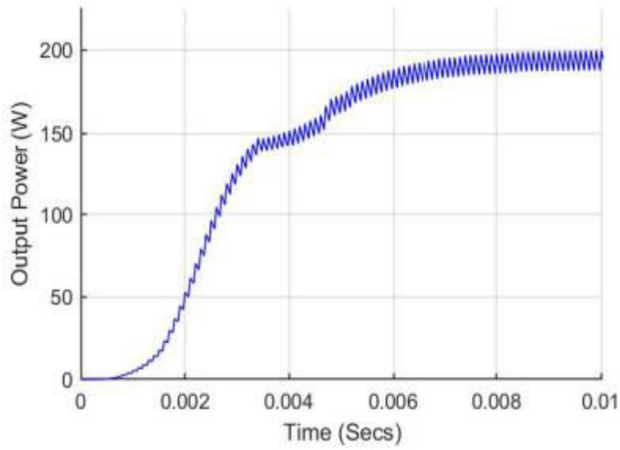

Figure-20. The zoomed image of the output power at 1000W/m^2.

In the simulations carried out in this work, the advanced fuzzy logic was used under the different influences of climatic conditions (lighting and temperature), which shows that it is accurate and robust. This algorithm can work at the optimal point without oscillations. It is characterized by good behavior as a transition state. This algorithm strongly depends on the rule base and the inference engine. The maximum point tracking with fuzzy logic has a fast response speed with a very low ripple and a fast settling time. Finally, the proposed advanced model was evaluated based on the efficiency criteria [23]. It is calculated using the following equation:

$$\eta = \frac{P_{load}}{P_{pv}} \quad (16)$$

Table-3 below shows the full results of the simulation with variable illumination at a temperature of 25°C.

Table-3. Results of the output power of the converter at variable light and fixed temperature.

Illumination (W/m^2)	1000	900	800	700	600
T(°C)	25	25	25	25	25
V_{pv} (V)	28.7	28.69	28.92	28.99	28.99
V_{out} (V)	109.03	103.56	97.80	91.55	84.66
D_{MPP} (%)	73.7%	72.3%	70.4%	68.3%	65,6%
Ppv (W)	200	180.9	161.5	141.8	121.9
P_{Load} (W)	198.2	178.5	159.1	139.7	119.4
Oscillation(W)	12	10	8.4	7.4	6.4
Efficiency (%)	99.1%	98.6%	98.5%	98.5%	98%

- The duty cycle D is calculated as follows:

$$D = 1 - \frac{V_{int}}{V_{out}} \quad (17)$$

5.2 Results with Varying Temperature at an Illumination of 1000W/m^2

In the following, the behavior of the advanced controller FL is studied with a rapid temperature increase from 15°C to 35°C and a temperature decrease from 35°C to 15°C at a fixed illuminance of 1000W/m^2. The system converges rapidly with low ripple and very low overshoot as shown in (Figures 22, 23, 24, 25, 26, & 27).

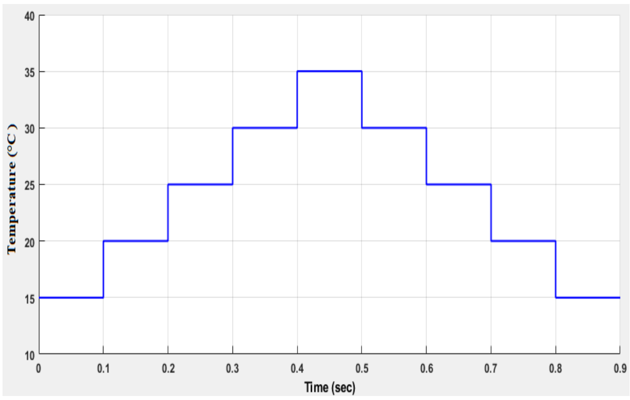

Figure-21. Change of temperature at 1000W/m^2.

VOL. 17, NO. 24, DECEMBER 2022 ISSN 1819-6608
ARPN Journal of Engineering and Applied Sciences

www.arpnjournals.com

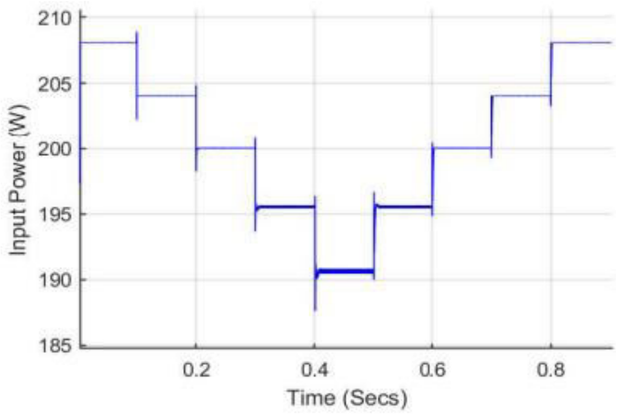

Figure-22. Input power at 1000W/m^2.

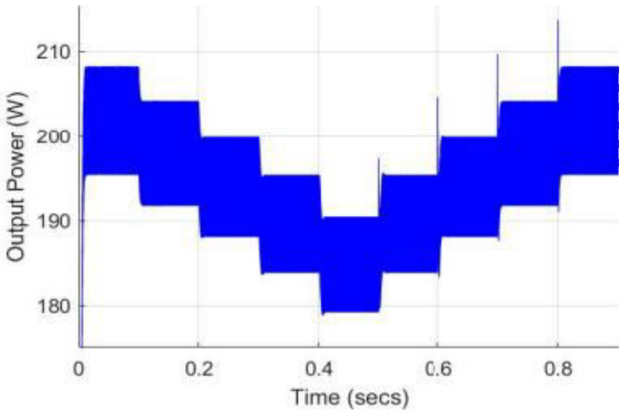

Figure-23. Output power at 1000W/m^2.

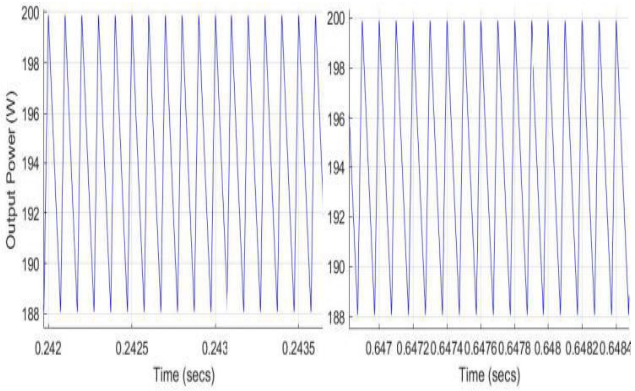

Figure-24. The zoomed image of the output power at 1000W/m^2 at 25°C.

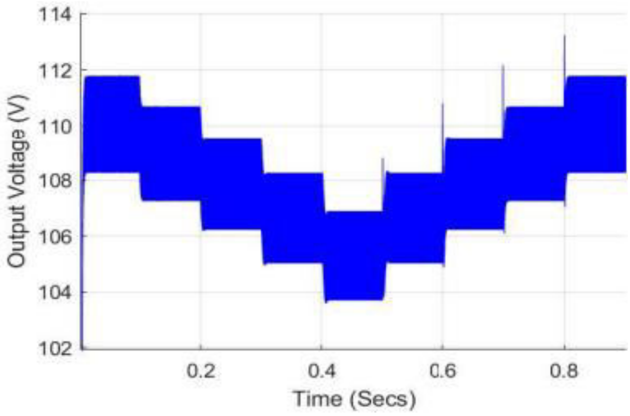

Figure-25. Output voltage at 1000W/m^2.

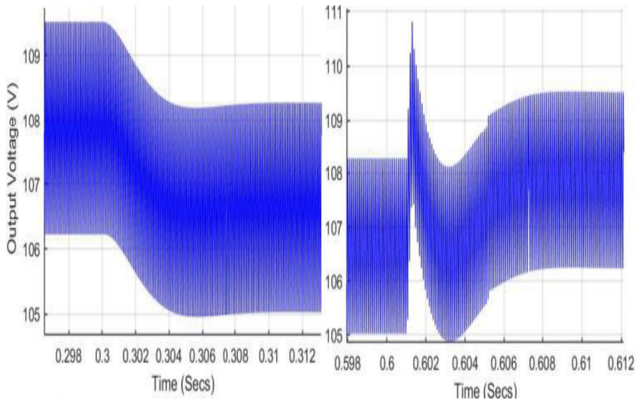

Figure-26. The zoomed image of the output voltage at 1000W/m^2.

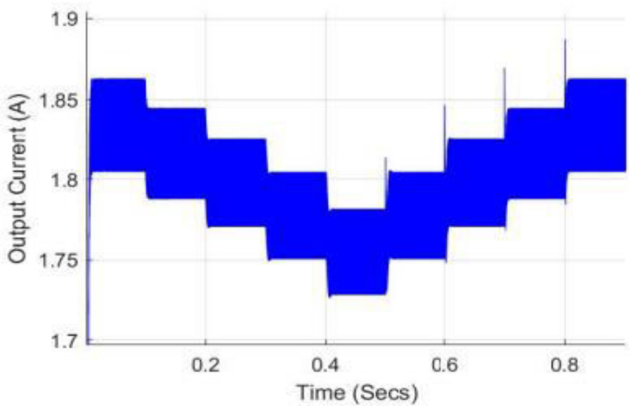

Figure-27. Output current at 1000W/m^2.

Table-4. Results of the output power of the converter at variable temperature and fixed light.

T (°C)	15	20	25	30	35
Illumination (W/m^2)	1000	1000	1000	1000	1000
V_{pv} (V)	30.02	29.37	28.7	28.04	27.39
V_{out} (V)	111.1	110.1	109	107.7	106.4
D_{MPP} (%)	73%	73.3%	73.7%	74%	74.2%
Ppv (W)	208.1	204.1	200	195.9	191.8
P_{Load} (W)	206.3	202.4	198.2	193.7	188.7
Oscillation (W)	12	12	12	11.5	11.2
Efficiency (%)	99.1%	99.1%	99.1%	98.9%	98.4%

Through this comprehensive study and analysis, the results obtained show us how efficient and powerful the advanced fuzzy logic controller is to achieve a stable maximum power point in a short time, with an improved efficiency of up to 99.1% with a very fast settling time of 4 ms, and very low overshoot.

6. CONCLUSIONS

In this paper, the simulations performed with the fuzzy logic method for photovoltaic systems under different weather conditions have shown that the results obtained with the advanced fuzzy controller are efficient and robust, with excellent accuracy and reliability in the face of a rapid change in illumination and temperature, without power losses due to the oscillation of the operating point of the system around its optimal position and a long transition regime.

The proposed system and control method can help to ensure the maximum power point tracking to a stable value with fast settling time, very low overshoot, and improved efficiency of up to 99.1%.

REFERENCES

[1] B. Meryem, Naddami Ahmed, Fahli Ahmed. 2019. Photovoltaic Power Control using Fuzzy Logic and Fuzzy Logic Type 2 MPPT Algorithms and Buck Converter. Advances in Technology Innovation. 4(3): 125-139

[2] A. Pradhan, B. Pand. 2018. A Simplified Design and Modeling of Boost Converter for Photovoltaic System. International Journal of Electrical and Computer Engineering (IJECE), 8(1): 141-149, February 2018. doi: 10.11591/ijece.v8i1.pp141-149

[3] S. A. Mohamed, M. Abd El Sattar. 2019. A comparative study of P&O and INC maximum power point tracking techniques for grid-connected PV systems. Springer Nature Switzerland Applied Sciences. 1, 174. doi: 10.1007/s42452-018-0134-4

[4] S. Yaqin, G. Tingkun, D. Yan, Z. Linghan and T. Jingxuan. 2018. Photovoltaic array maximum power point tracking based on improved perturbation and observation method. Journal of Physics: Conference Series. 1087: 1-6. doi: 10.1088/1742-6596/1087/4/042079

[5] A. Ilyas, M. Ayyub, M. R. Khan, A. Jain, and M. A. Husain. 2017. Realization of incremental conductance the MPPT algorithm for a solar photovoltaic system. International Journal of Ambient Energy. 39(8): 873-884. doi: 10.1080/01430750.2017.1354322

[6] U. Yilmaz, A. Kircay and S. Borekci. 2018. PV system fuzzy logic MPPT method and PI control as a charge controller. Renewable and Sustainable Energy Reviews. 81: 994-1001. doi: http://dx.doi.org/10.1016/j.rser.2017.08.048

[7] M. R. Kumar, S. S. Narayana and G. Vulasala. 2018. Advanced sliding mode control for solar PV array with fast voltage tracking for MPP algorithm. International Journal of Ambient Energy. pp. 1-9. doi: https://doi.org/10.1080/01430750.2018.1492448

[8] A. Heinämäki, G. Guekos. 1987. Solar cell short circuit current dependence on the angle of the incident radiation. Solar Energy Materials and Solar Cells. 20(1): 65-73. Doi: https://doi.org/10.1016/0379-6787(87)90022-6

[9] A. A.Barakate, R. Abdelmoumene, A. Wahbi, M. Maddi, L. Hlou and A. Hadjoudja. 2021. Modelling, Development and Analysis Performance of An Intelligent Control of Photovoltaic System by fuzzy Logic Approach for Maximum Power Point Tracking. International Journal of Communication Networks and Information Security (IJCNIS). 13(1): 42-47.

[10] K.-H. Chao, L.-Y. Chang, K.-W. Wang. 2022. Global Maximum Power Point Tracking of Photovoltaic Module Arrays Based on Improved Cuckoo Search Algorithm. Electronics, 11, 1247. https://doi.org/10.3390/electronics11081247

[11] Rekioua D., Matagne E. 2012. Optimization of Photovoltaic Power Systems; Springer: London, UK, oi: 10.1007/978-1-4471-2403-0

[12] K. Ding, X. G. Bian, H. H. Liu, T. Peng. 2012. A MATLAB-Simulink-Based PV Module Model and its

Application Under Conditions of Nonuniform radiation. IEEE Trans. Energy Convers. 27, 864-872. Doi: 10.1109/TEC.2012.2216529

[13] Kabbani A. and Honnurvali M. S. (2021) PV Cell Parameters Modeling and Temperature Effect Analysis. International Journal of Renewable Energy Development, 10(3), 563-571., doi: https://doi.org/10.14710/ijred.2021.33845

[14] Y. Jiang, J. A. A. Qahouq, I. Batarseh. 2010. Improved solar PV cell MATLAB simulation model and comparison. In Proceedings of the 2010IEEE International Symposium on Circuits and Systems, Paris, France, 30 May–2 June; pp. 2770-2773. Doi:10.1109/ISCAS.2010.5537014

[15] M. G. Villalva, J. R. Gasol, E. R. Filho. 2009. Modelling and circuit-based simulation of photovoltaic arrays. In Proceedings of the 2009 Brazilian Power Electronics Conference, Bonito-Mato Grosso do Sul, Brazil, 27 September-1 pp. 1244-1254. Doi:10.1109/COBEP.2009.5347680

[16] Y. T. Tan, D. S. Kirschen, N. Jenkins. 2004. A Model of PV Generation Suitable for Stability Analysis. IEEE Trans. Energy Convers. 19, 748-755. doi: 10.1109/TEC.2004.827707

[17] R. Ayop and C. W. Tan. 2018. Design of boost converter based on maximum power point resistance for photovoltaic applications. Solar Energy. 160: 322-335. doi: 10.1016/j.solener.2017.12.016

[18] A. Pradhan, B. Panda. 2018. A Simplified Design and Modelling of Boost Converter for Photovoltaic Sytem. International Journal of Electrical and Computer Engineering. 8(1): 141-149. doi: 10.11591/ijece.v8i1.pp141-149

[19] Hassan M. H. Farh, Ali M. Eltamaly, Mamdooh Al Saud. 2019. Interleaved boost converter for global maximum power extraction from the photovoltaic system under partial shading. The institution of engineering and technology. doi: https://doi.org/10.1049/iet-rpg.2018.5256

[20] R. Abdelmoumene, A. A. Barakate, A. Wahbi, M. Omar, A. Benlafkih, A. Hadjoudja. 2022. A novel boost converter based fussy logic method for fast and accurate maximum power point tracking to control a stand-alone PV system. ARPN Journal of Engineering and Applied Sciences. 17(6): 621-629.

[21] A. Rezvani, M. Gandomkar. 2016. Modelling and control of grid connected intelligent hybrid photovoltaic system using new hybrid fuzzy-neural method. Sol Energy; 127: 1-18. Doi: https://doi.org/10.1016/j.solener.2016.01.006

[22] R. Rajesh, M. C. Mabel. 2014. Efficiency analysis of a multi-fuzzy logic controller for the determination of operating points in a PV system. Sol Energy; 99: 77-87. doi: 10.1016/j.solener.2013.10.036

[23] S. Rama Phanindra Chitturi, *et al*. 2018. Efficiency of photovoltaic systems in mountainous areas. IEEE International Energy Conference (ENERGYCON), doi: 10.1109/ENERGYCON.2018.8398766